Postsynthetic Bromination of UiO-66 Analogues: Altering Linker Flexibility and Mechanical Compliance

Ross J. Marshall,[a] Tom Richards,[b] Claire Hobday,[c] Colin F. Murphie,[a] Claire Wilson,[a] Stephen A. Moggach,[c] Thomas D. Bennett,[b]* and Ross S. Forgan[a]*

[a] *WestCHEM, School of Chemistry, The University of Glasgow, University Avenue, Glasgow G12 8QQ, UK.*
E-mail: Ross.Forgan@glasgow.ac.uk
www.forganlab.com

[b] *Department of Materials Science and Metallurgy, University of Cambridge, Cambridge CB3 0FS, UK.*
E-mail: tdb35@cam.ac.uk

[c] *EaStCHEM, School of Chemistry, University of Edinburgh, Joseph Black Building, West Mains Road, Edinburgh, EH9 3JJ, UK.*

SUPPORTING INFORMATION

Table of Contents:

S1.	**General Experimental Remarks.**	**S2**
S2.	**Synthesis.**	**S3**
S3.	**Postsynthetic Bromination of (2).**	**S8**
S4.	**^{13}C NMR Spectra of Digested (2) and (2-Br$_2$).**	**S10**
S5.	**Pore Size Distribution.**	**S11**
S6.	**Nanoindentation.**	**S12**
S7.	**Attempted Synthesis of the Zr MOF Containing etdb.**	**S13**
S8.	**References.**	**S15**

S1. General Experimental Remarks

All chemicals and solvents were purchased from Alfa Aesar, Fisher Scientific, Fluorochem, Merck, Sigma-Aldrich, Strem Chemicals and VWR and used without further purification.

Microwave Synthesis: Microwave reactions were carried out in 35 ml pressure vials using a CEM Discover SP microwave, equipped with an Explorer 12 Hybrid autosampler. The power was allowed to fluctuate to maintain a constant temperature of 100 °C throughout the course of the reaction. (University of Glasgow)

Powder X-ray Diffraction (PXRD): PXRD measurements were carried out at 298 K using a PANalytical X'Pert PRO diffractometer (λ (CuKα) = 1.4505 Å) on a mounted bracket sample stage. Data were collected over the range 3 – 45 °. PXRD patterns were calculated from single crystal data using Mercury 3.5.1.[S1] (University of Glasgow)

Single Crystal Diffraction (SCXRD): Data for **(2)** were collected on a Bruker Apex II (λ (MoKα = 0.71073 Å) diffractometer (University of Edinburgh). Data for **(etdb-Me_2)** were collected on a Bruker Apex II (λ (MoKα = 0.71073 Å) diffractometer equipped with an Oxford Cryosystems n-Helix device (University of Glasgow). Data for **(2-Br_2)** were collected using a Rigaku AFC12 goniometer equipped with an enhanced sensitivity (HG) Saturn724+ detector mounted at the window of an FR-E+ SuperBright molybdenum rotating anode generator with VHF Varimax optics (70 μm focus) equipped with an Oxford Cryosystems cryostream device. (EPSRC UK National Crystallography Service)

Thermal Gravimetric Analysis (TGA): Measurements were carried out using a TA Instruments Q500 Thermogravimetric Analyser. Measurements were collected from room temperature to 1000 °C with a heating rate of 10 °C / min under an N_2 atmosphere. (University of Glasgow)

Nuclear Magnetic Resonance (NMR): NMR spectra were recorded on either a Bruker AVIII 400 MHz spectrometer or a Bruker AVI 500 MHz Spectrometer and referenced to residual solvent peaks. (University of Glasgow)

Gas Uptake: N_2 adsorption isotherms were carried out at 77 K on a Quantachrome Autosorb iQ gas sorption analyser. Samples were degassed under vacuum at 120 °C for 20 h using the internal turbo pump. BET surface areas were calculated using the Micropore BET Assistant and pore size distribution analysis was carried out using QSDFT (N_2 on carbon at 77 K, slit/cylindrical pore model) both implemented in the Quantachrome ASiQwin operating software. (University of Glasgow)

Nanoindentation: Nanoindentation was performed under ambient conditions using an MTS Nanoindenter XP. Samples were mounted in an epoxy resin and polished using increasingly fine diamond suspensions. (University of Cambridge)

S2. Synthesis

The chemical structures and abbreviated names of all ligands used in this study – generated postsynthetically or otherwise – are detailed in Scheme S1. All ligands and precursors were purchased from chemical suppliers, unless otherwise stated.

	R	Compound	Isomerism?
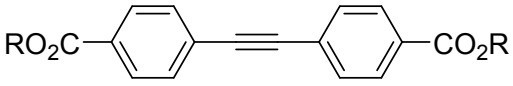	CH_3	edb-Me_2	n/a
	H	edb-H_2	
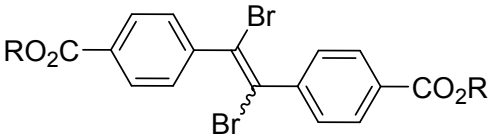	CH_3	edb-Br_2-Me_2	*cis*/*trans*
	H	edb-Br_2-H_2	
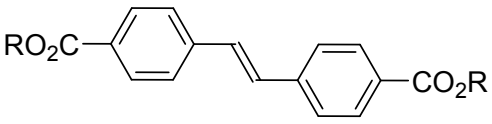	CH_3	sdc-Me_2	n/a
	H	sdc-H_2	
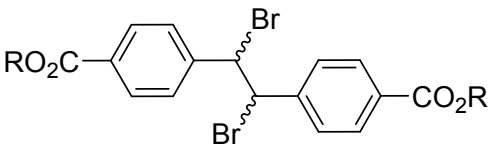	CH_3	sdc-Br_2-Me_2	(*RR*)/(*SS*)/*meso*
	H	sdc-Br_2-H_2	
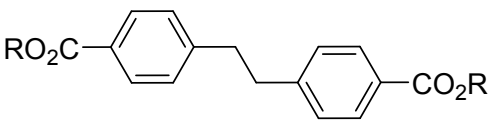	Me	etdb-Me_2	n/a
	H	etdb-H_2	

Scheme S1. Chemical structures of compounds and the abbreviation scheme used in this study.

The alkyne-bridged ligand, 4,4′-ethynylenedibenzoic acid (edb-H_2), was prepared as described previously from its dimethyl ester.[S2] The ligand 4,4′-ethane-1,2-diyldibenzoic acid (etdb-H_2) and its methyl ester were synthesised according to modified literature procedures.[S3]

etdb-Me_2

Dimethyl *trans*-stilbene-4,4'-dicarboxylate (0.500 g, 1.69 mmol) was dissolved in methanol (25 ml) by stirring. Palladium on carbon (10 %, 0.075 g) was added, and the solution was degassed by bubbling N_2 through the solution for 10 minutes. The reaction flask was purged with H_2, before being left to stir at room temperature overnight under H_2 atmosphere. The mixture was filtered through Celite and washed through with excess methanol. The solvent was removed under reduced pressure to yield a white solid (0.454 g, 1.52 mmol, 90 %). ^{1}H NMR (DMSO-d_6): δ/ppm 2.99 (s, 4H), 3.83 (s, 6H), 7.36 (d, 4H, J = 8.2 Hz), 7.86 (d, 4H, J = 8.2 Hz); ^{13}C NMR (DMSO-d_6): δ/ppm 36.3 (CH_2), 52.0 (CH_3), 127.4 (C), 128.9 (CH), 129.2 (CH), 147.0 (C), 166.2 (C); HRESIMS calculated for $C_{18}H_{18}O_4$ $(M)^+$ 298.1205, found *m/z* 298.1209.

Single crystals of etdb-Me_2 were serendipitously isolated after evaporation of a methanolic solution, mounted in inert oil and transferred to the cold gas stream of the diffractometer. A representation of the molecule from its crystal structure is shown in Figure S1.

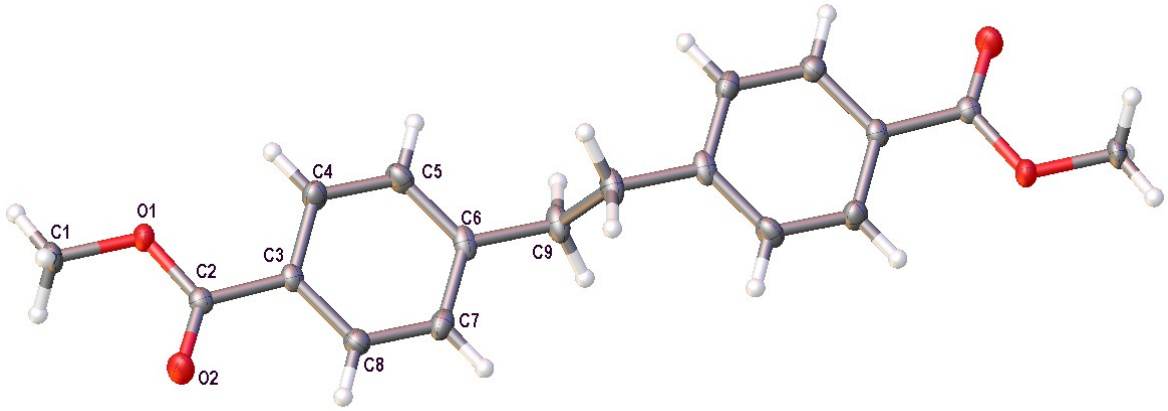

Figure S1. View showing the molecular structure in the crystal and atom labelling scheme (asymmetric unit only) for **etdb-Me_2**, displacement ellipsoids drawn at 50% probability level.

Crystal Data for etdb-Me$_2$. $C_{18}H_{18}O_4$, M_r = 298.32, Monoclinic, a = 4.7414 (4) Å, b = 6.0450 (6) Å, c = 25.976 (2) Å, β = 94.197 (4)°, V = 742.53 (12) Å^3, T = 100 K, space group $P2_1/n$ (no. 14), Z = 2, 10757 reflections measured, 1667 unique (R_{int} = 0.074), which were used in all calculations. The final R_1 = 0.059 for 1465 observed data [$F^2 > 2s(F^2)$] and $wR_2(F^2)$ = 0.160 (all data).

Single crystal diffraction data for **etdb-Me$_2$** were collected and processed using a Bruker Apex,[S4] and a multi-scan absorption correction was made using SADABS.[S5] The structure was solved by charge-flipping methods using SuperFlip[S6] and refined against F^2 using full-matrix least-squares refinement using SHELX2014[S7] within OLEX2.[S8] Positional and anisotropic atomic displacement parameters (adps) were refined for all non-hydrogen atoms. Hydrogen atoms were placed at calculated positions and refined as part of a riding model for the phenyl hydrogens and as a rigid rotor for the methyl hydrogens. The molecule crystallises across an inversion centre, with half the molecule in the asymmetric unit and the other half generated through inversion symmetry.

<u>etdb-H$_2$</u>

Dimethyl 4,4′-ethane-1,2-diyldibenzoate (0.383 g, 1.28 mmol, 1 eq) was dissolved in ethanol (50 ml) by stirring. Potassium hydroxide (0.372 g, 6.63 mmol, 5 eq) was dissolved separately in H_2O (50 ml), then the two solutions were combined and subject to reflux overnight. The product was precipitated by addition of 1 M aqueous HCl, collected by filtration, washed with excess water until neutral and dried in a desiccator under vacuum (0.330 g, 1.22 mmol, 95%). ^{1}H NMR (DMSO-d_6): δ/ppm 2.97 (s, 4H), 7.34 (d, 4H, J = 8.3 Hz), 7.84 (d, 4H, J = 8.3 Hz), 12.82 (s, 2H); ^{13}C NMR (DMSO-d_6): δ/ppm 36.4 (CH_2), 128.5 (C), 128.6 (CH), 129.3 (CH), 146.5 (C), 167.3 (C); HRESIMS calculated for $C_{16}H_{13}O_4$ $(M-H)^-$ 269.0819, found *m/z* 269.0815.

Single crystal samples of $[Zr_6O_4(OH)_4(edb)_6]_n$ **(1)** and $[Zr_6O_4(OH)_4(trans\text{-}edb\text{-}Br_2)_6]_n$ **(1-Br$_2$)** were prepared according to our previously reported methods.[S9] The syntheses of the analogous Zr MOF $[Zr_6O_4(OH)_4(sdc)_6]_n$ **(2)** and its postsynthetic brominated derivative $[Zr_6O_4(OH)_4(sdc\text{-}Br_2)_6]_n$ **(2-Br$_2$)** were carried out using the same protocols.

Bulk Material **(2)**

L-proline (0.518 g, 4.50 mmol 5 eq), 4,4′-stilbenedicarboxylic acid (0.241 g, 0.90 mmol, 1 eq) and zirconium chloride (0.210 g, 0.90 mmol, 1 eq) were added to a 35 ml microwave vial. DMF (20 ml) was added, followed by hydrochloric acid (0.08 ml) and the vial was sealed. The reaction vessel was then subject to an automated microwave programme consisting of 10 minutes of stirring at 30 °C to homogenously distribute the reagents, followed by heating at 100 °C for 4 hours without stirring. The bulk material was collected from the vial upon completion, centrifuged once with fresh DMF and three times with acetone, before being placed in a desiccator under vacuum for drying (0.289 g, 0.13 mmol, 87 % - average yield over 4 reactions). Bromine analysis: 0% (calc); 0.8% (found).

Activation: Powder samples were added to 50 ml PYREX reagent bottles and left to stand in $CHCl_3$, for activation under conditions comparable to the bulk brominated MOF **(2-Br$_2$)** *vide infra*. The $CHCl_3$ was exchanged for fresh $CHCl_3$ a further 2 times over 48 hours, before being collected by centrifugation and placed in a desiccator under vacuum for drying.

Single Crystals **(2)**

L-proline (0.104 g, 0.90 mmol, 4 eq), 4,4′-stilbenedicarboxylic acid (0.060 g, 0.23 mmol, 1 eq) and zirconium chloride (0.052 g, 0.23 mmol, 1 eq), were added to a 50 ml PYREX reagent bottle. To the bottle DMF (10 ml) was added, followed by sonication for 10 minutes. Hydrochloric acid (0.02 ml) was added, and the mixture was sonicated for a further 10 minutes, followed by heating at 100 °C for 48 hours in the oven. The bottles were removed from the oven after this period, and allowed to cool to room temperature. The crystals were left to stand in their mother solution.

Crystal Data for (2): $Zr_6O_4(OH)_4(C_{16}H_{10}O_4)_6$, M_r = 3235.71, Cubic, a = 29.8884 (3) Å, V = 26699.9 (8) Å^3, T = 100 K, space group *Fm*-3*m* (no. 225), Z = 4, 95174 reflections measured, 1235 unique (R_{int} = 0.068), which were used in all calculations. The final R_1 = 0.0761 for 951 observed data [F> 2s(F)] and $wR_2(F)$ = 0.0871 (all data).

Single crystal X-ray diffraction data were collected and processed with CrysalisPro.[S10] The structure was solved by charge-flipping methods using SuperFlip and refined against F^2 using all data using CRYSTALS.[S11] Using the SQUEEZE algorithm within PLATON,[S12] the pore volume and electron density within the voids were calculated and found to be 17550 Å^3 and

5529 electrons per unit cell (the equivalent of ~138 molecules of DMF) respectively. During refinement of data all non-hydrogen atoms were refined anisotropically, with the exception of C(30), C(31), C(40) and C(41) with thermal similarity and vibrational restraints applied to all non-hydrogen atoms except Zr. 1,2 and 1,3 distances on the sdc^{2-} were restrained, while a planarity restraint was applied to the phenyl ring. Hydrogen atoms attached to C-atoms and the hydroxyl O-atom were placed geometrically and not refined.

The benzene ring is disordered over 3 positions in the ligand, the ring which sits in the plane of the ligand is occupied 50% of the time and the other two positions above and below the plane occupied 25 % each. (Figure S1). Site-occupied disorder for C(6) results in 4 possible positions for the C=C bond linking across the two phenyl groups. Similar disorder was seen previously in the crystal structure of **(1-Br$_2$)**.[S9] In addition to the disorder of the linker, there is a hydroxide/oxide 50:50 disorder on the $Zr_6O_4(OH)_4$ core, which must be present in order for the framework to charge balance (see Figure S2). This type of disorder is not uncommon in UiO-framework materials.

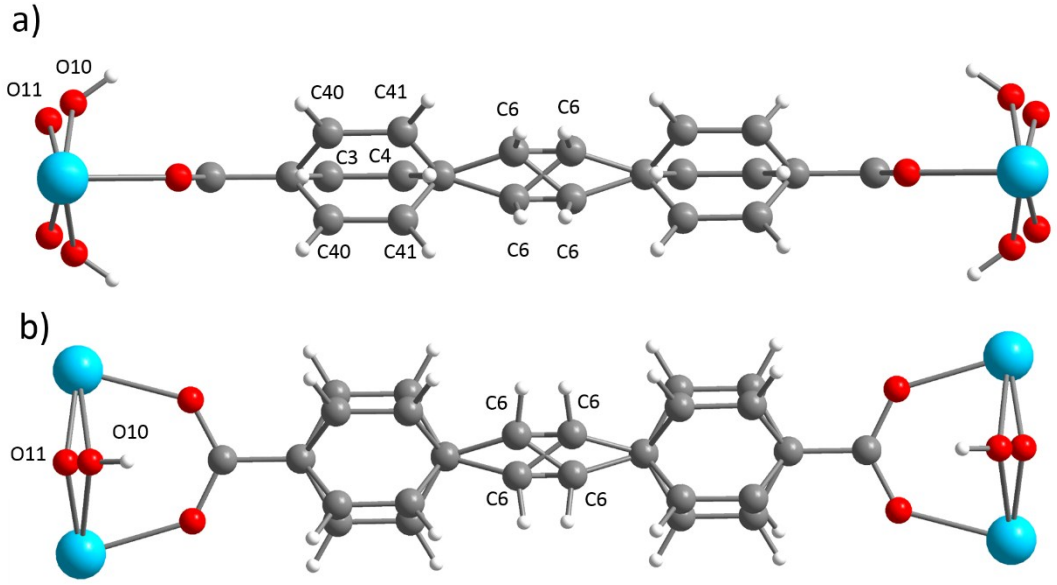

Figure S2. Disorder in the crystal structure of (**2**). **a)** Side on view of linker showing rotational disorder of the benzene rings within the ligand. View looking through the plane of the 50 % occupied C2-C3-C4-C5 ring with the other two 25 % occupied orientations above and below the plan. Also, four of the C6 positions can be observed. In addition a clear view of the hydroxide/oxide disorder on the $Zr_6O_4(OH)_4$ cluster. **b)** Above view of the linker, looking into the plane of the 50 % occupied C2-C3-C4-C5, with the other four C6 positions clearly visible.

With the solid-state structure of **(2)** to hand, the purity of the bulk samples could be assessed by powder X-ray diffraction; comparing experimental patterns to that derived from the crystal structure (Figure S3) showed an excellent match, indicating phase purity.

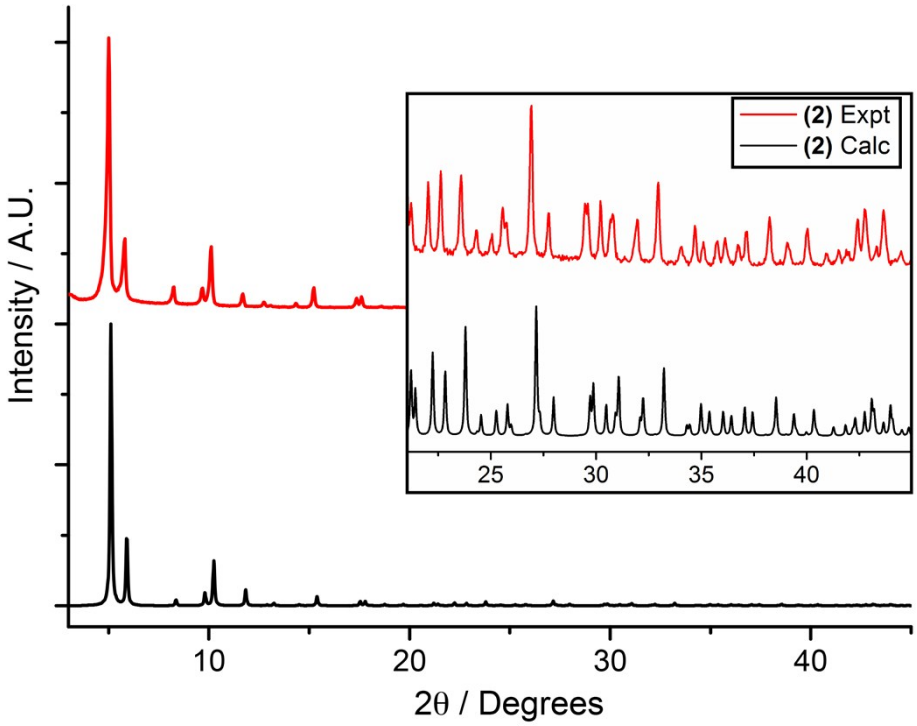

Figure S3. Calculated and experimental powder X-ray diffraction patterns of **(2)**.

S3. Postsynthetic Bromination of (2)

Bulk Material

Bulk powder of **(2)** (0.150 g, 0.40 mmol double bond, 1 eq) was added to a 50 ml reagent bottle and left to stand in 15 ml $CHCl_3$ overnight. The $CHCl_3$ was removed and fresh $CHCl_3$ added, followed by the addition of bromine (101 µl, 1.98 mmol, 5 eq). The bottle was sealed and stored in the dark for a period of 48 hours. The reaction product **(2-Br$_2$)** $[Zr_6O_4(OH)_4(sdc\text{-}Br_2)_6]_n$ was collected by centrifugation and washed multiple times with fresh $CHCl_3$, before being placed in a desiccator under vacuum for drying. Bromine analysis: 29.6% (calc); 27.7% (found).

Single Crystals

Small quantities of **(2)** were added by pipette to a vial containing fresh DMF. The DMF was replenished for fresh DMF twice before being exchanged for $CHCl_3$. The $CHCl_3$ was exchanged for fresh $CHCl_3$ a further two times. Bromine (13 µl, 0.26 mmol) was added, the vial was sealed and left to stand in the dark for 48 hours. The $CHCl_3$ was replenished multiple times for fresh $CHCl_3$. A small portion of the crystals of **(2-Br$_2$)** $[Zr_6O_4(OH)_4(sdc\text{-}Br_2)_6]_n$ were added to a vial containing fresh DMF. After 24 h the DMF was exchanged for fresh DMF and the crystals left to stand.

Single Crystal Data for **(2-Br$_2$)**: $Zr_6O_4(OH)_4(C_{16}H_{10}O_4Br_2)_6$, M_r = 3235.71, Cubic, a = 29.7685 (8) Å, V = 26380 (2) Å^3, T = 100 K, space group Fm-3m (no. 225), Z = 4, 95174 reflections measured, 1211 unique (R_{int} = 0.088), which were used in all calculations. The final R_1 = 0.084 for 1075 observed data [$F^2 > 2s(F^2)$] and $wR_2(F^2)$ = 0.268 (all data).

Single crystal X-ray diffraction data were collected and processed using CrystalClear.[S13] The structure was solved by charge-flipping methods using SuperFlip[S6] and refined against F^2 using full-matrix least-squares refinement using SHELX2014[S7] within OLEX2.[S8] SQUEEZE within PLATON[S12] was used to identify solvent accessible voids of 18145 Å^3 which contain 3735 electrons per unit cell (which corresponds to ~93 molecules of DMF). Positional and anisotropic atomic displacement parameters (adps) were refined for Zr, O and Br atoms, C atoms were refined with isotropic adps with distance restraints applied to the C-C distances and rigid body restraints applied to the anisotropic adps and similarity restraints to adps for all adjacent atoms. Hydrogen atoms were placed in geometrically calculated positions for the aromatic CH and refined as part of a riding model with U(iso)H = 1.2 U(eq) of the parent atom. OH hydrogen atoms and the CH atoms bound to C6 were not included explicitly in the model but are included in the cell contents and all values derived from them.

The ring has been modelled over 2 half occupied orientations with C3X and C4Y in general positions with distance and planarity restraints applied; C6 was modelled over four symmetry related 0.25 occupied sites and Br1 site is chemically fully occupied (0.25 crystallographically) but corresponds to a common site of attachment from all C6 positions. The two orientations/disorder components are 38° apart. The BrC-CBr plane lies at approximately 75 or 105° to the plane of the rings C2-C5. A view showing a single

orientation of central part of the linker with the independent atom sites labelled and a view showing the disorder components are shown in Figure S4.

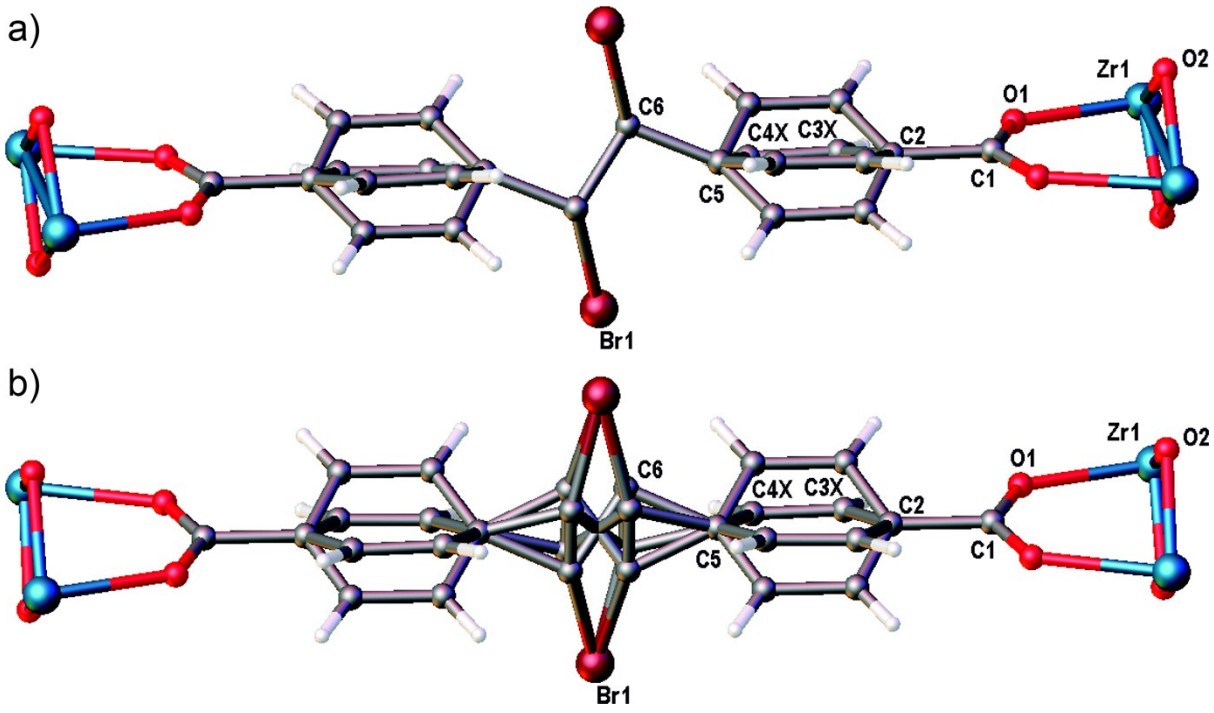

Figure S4. Disorder of the sdc-Br_2^{2-} linker in the crystal structure of **(2-Br_2)**. **a)** Disorder of the phenyl rings only, for clarity, and **b)** disorder across the linker.

S4. ^{13}C NMR Spectra of Digested (2) and (2-Br_2)

The bromination process was easily monitored by NMR spectra of samples of the MOFs digested in a mixture of D_2SO_4 and DMSO-d_6. The ^{1}H NMR spectra of digests of **(2)** and **(2-Br_2)** are discussed in the main text, and show easily identifiable shifts in the resonances assigned to the protons around the alkene / bromoalkane bridges. Similarly, the signals assigned to the carbon atoms in the ligand bridges shift dramatically in the ^{13}C NMR spectra (Figure S5). The resonance of the alkenyl carbon atom in digested samples of **(2)**, found at δ = 130.9 ppm and unambiguously assigned by DEPT spectra, is dramatically shifted upfield upon bromination, and in **(2-Br_2)** is found at δ = 54.1 ppm. This large change in chemical shift is a consequence of the change in hybridisation of the carbon atom, from sp^2 in a fully

conjugated system in **(2)** to sp^3 in **(2-Br$_2$)**, and the electronic effect of the electronegative bromine atom. In concert with the ^{1}H NMR spectra, the ^{13}C NMR spectra clearly show quantitative bromination of **(2)**.

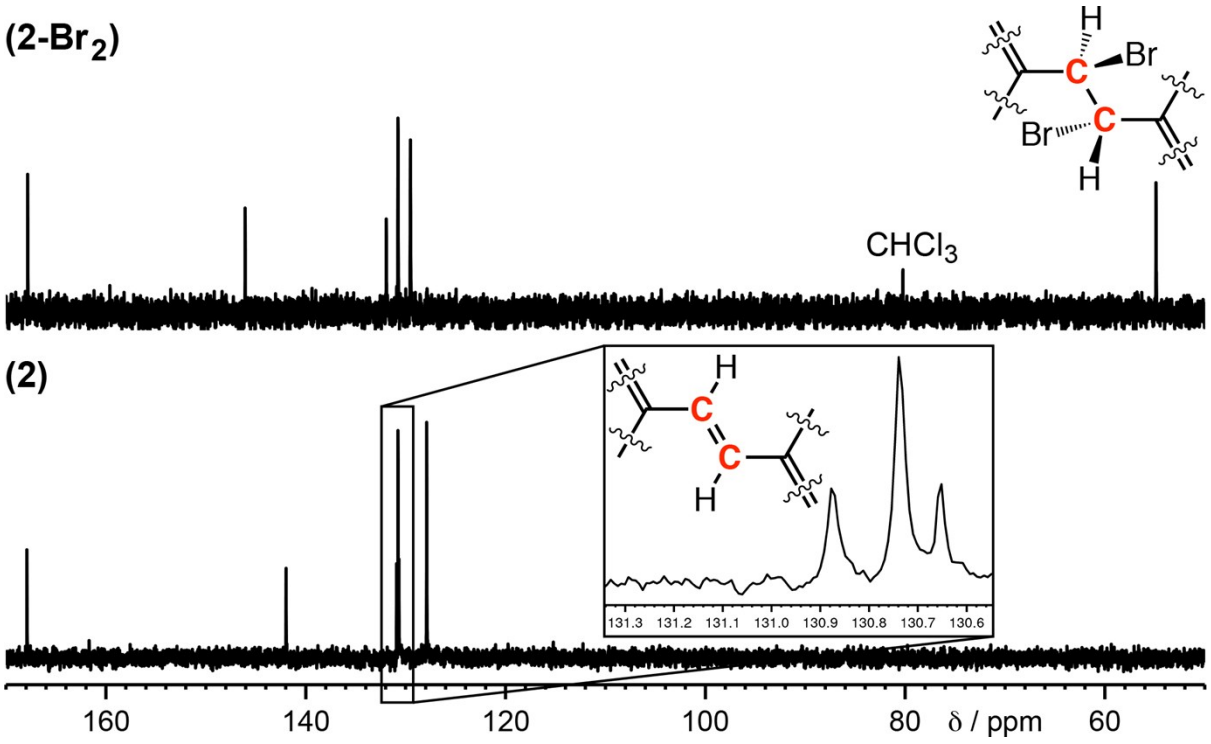

Figure S5. Stacked ^{13}C NMR spectra (D_2SO_4/DMSO-d_6, 293 K) of digested samples of **(2)** and **(2-Br$_2$)**. The resonance assigned to the alkenyl carbon atom of **(2)**, found at δ = 130.9 ppm, is dramatically shifted to δ = 54.1 ppm on conversion to the bromoalkane functionality in **(2-Br$_2$)**.

S5. Pore Size Distributions

The bulk samples of **(2)** and **(2-Br$_2$)** were further activated by evacuation under vacuum (internal turbo pump) at 120 °C for 20 h prior to BET analysis through N_2 adsorption isotherms at 77 K. The BET surface areas calculated from the isotherms show a decrease as a consequence of bromination, from 2900 m^2g^{-1} for **(2)** to 1580 m^2g^{-1} for **(2-Br$_2$)**. The decreases in surface area after bromination (45.5%) cannot be simply accounted for by the increase in mass as a result of incorporation of bromine – the decrease is too substantial – and so the isotherms clearly show a decrease in surface area as a consequence of the expected

mechanical contraction that bromination induces. The contraction of the frameworks is evident in the pore size distributions (Figure S6), which show a decrease in the main pore diameter from ~11.9 Å for **(2)** to ~10.1 Å for **(2-Br$_2$)** as a result of the mechanical contraction.

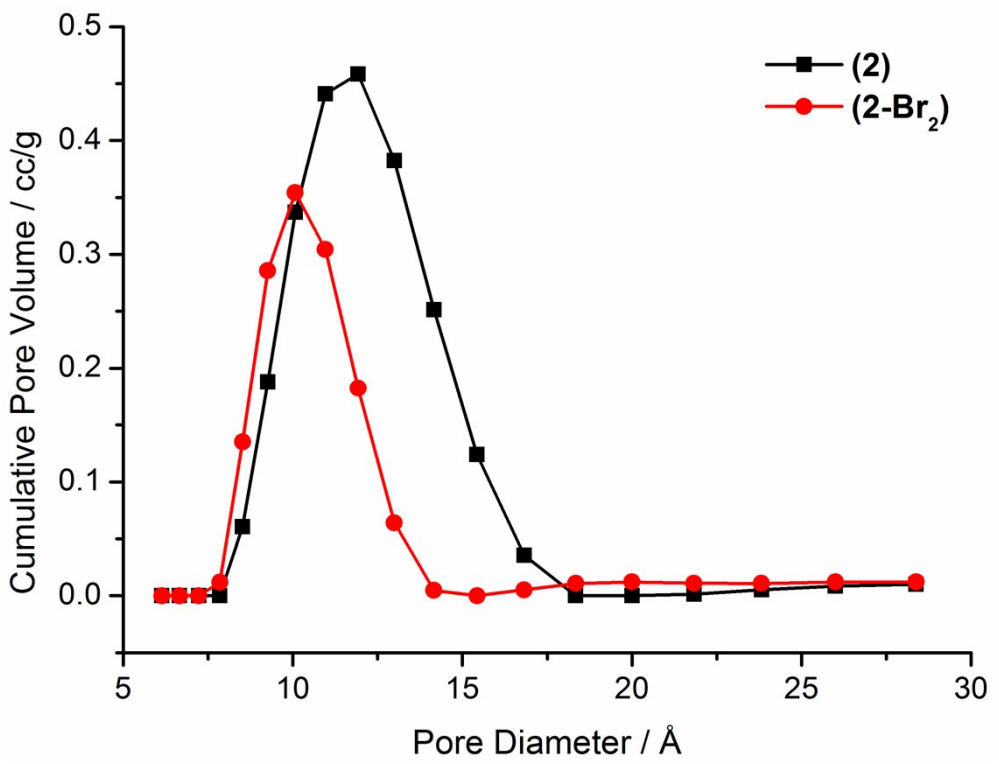

Figure S6. Comparison of the pore size distributions calculated from the N_2 adsorption isotherms using QSDFT of **(2)** vs **(2-Br$_2$)**.

S6. Nanoindentation

Indentation experiments were performed under the dynamic displacement controlled mode, at a constant strain rate of 0.05 s^{-1}. All tests were conducted using a three-sided pyramidal (Berkovich) diamond indenter tip, to a maximum surface penetration depth of 500 nm. The load-displacement data collected were analysed using the Oliver & Pharr method.[S14] Data below 100 nm were disregarded due to surface effects. From the plots of load displacement versus indentation depth (Figure S7a), values of elastic moduli (reported in the main text) and hardness (Figures S7b, S7c) of the MOFs can be extracted.

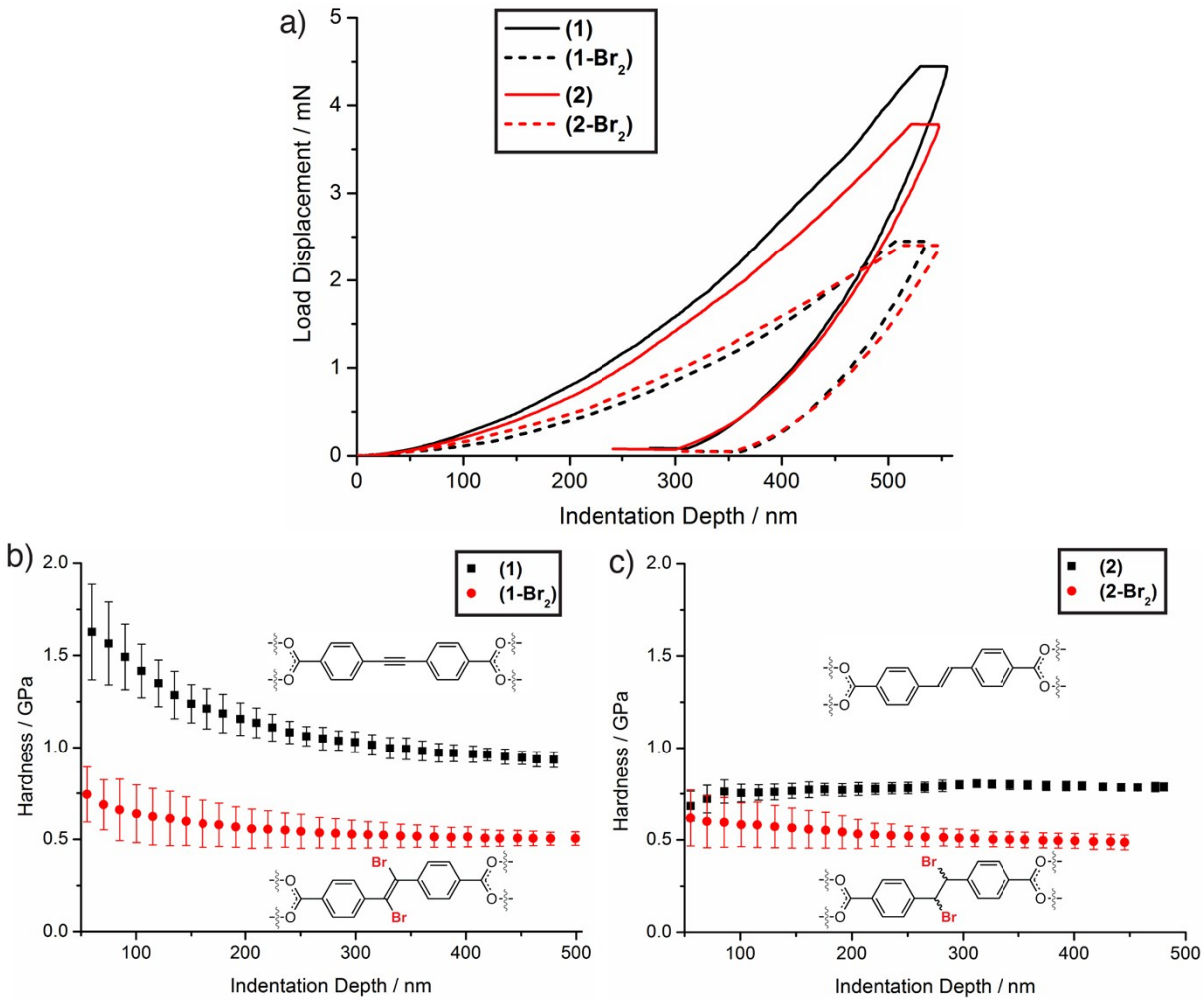

Figure S7. a) Load vs displacement curves for all four MOFs from nanoindentation experiments. Comparison of hardness as a function of depth for **b) (1)** vs **(1-Br$_2$)** and **c) (2)** vs **(2-Br$_2$)**, showing in both cases bromination results in a reduced hardness. Error bars are taken from an average of 15 indentations.

S7. Attempted Synthesis of the Zr MOF Containing etdb

Several attempts were directed towards the synthesis of a Zr MOF containing etdb, with conditions similar to the bulk synthesis of **(2)**, using L-proline modulation, used as a starting point. Alternatively, unmodulated syntheses, as well as conventional acetic and benzoic acid modulated methods were used to further investigate if this highly flexible ligand would be

incorporated within the typical UiO topology. Conventional and microwave heating protocols were also attempted, with synthetic conditions detailed below.

Microwave Synthesis

L-proline (0.130 g, 1.13 mmol 5 eq), 4,4′-ethane-1,2-diyldibenzoic acid (0.061 g, 0.23 mmol, 1 eq) and zirconium chloride (0.52 g, 0.23 mmol, 1 eq) were added to a 35 ml microwave vial. DMF (10 ml) was added, followed by hydrochloric acid (0.02 ml) and the vial was sealed. The reaction vessel was then subject to an automated microwave programme consisting of 10 minutes of stirring at 30 °C to homogenously distribute the reagents, followed by heating at 100 °C for 4 hours without stirring. The powder was collected from the vial upon completion, centrifuged once with fresh DMF and two times with acetone, before being placed in a desiccator under vacuum for drying.

Oven Synthesis

Either L-proline (0.130 g, 1.13 mmol, 5 eq), acetic acid (0.064 ml, 1.13 mmol, 5 eq), benzoic acid (0.137 g, 1.13 mmol, 5 eq) or no modulator in the case of the unmodulated synthesis, as required, along with 4,4′-ethane-1,2-diyldibenzoic acid (0.061 g, 0.23 mmol, 1 eq) and zirconium chloride (0.052 g, 0.23 mmol, 1 eq) were added to a 50 ml PXREX reagent bottle. DMF (10 ml) was added, followed by hydrochloric acid (0.02 ml) and the vial was sealed. The reaction vessel was then subject to sonication to aid homogenous distribution of the reagents, followed by heating at 120 °C for 24 hours in the oven. The powder was collected from the bottle upon completion, centrifuged once with fresh DMF and two times with acetone, before being placed in a desiccator under vacuum for drying.

Powder X-ray diffraction analyses of the resulting precipitates clearly show that synthesis of a crystalline MOF was unsuccessful, with only amorphous materials present (Figure S8, overleaf).

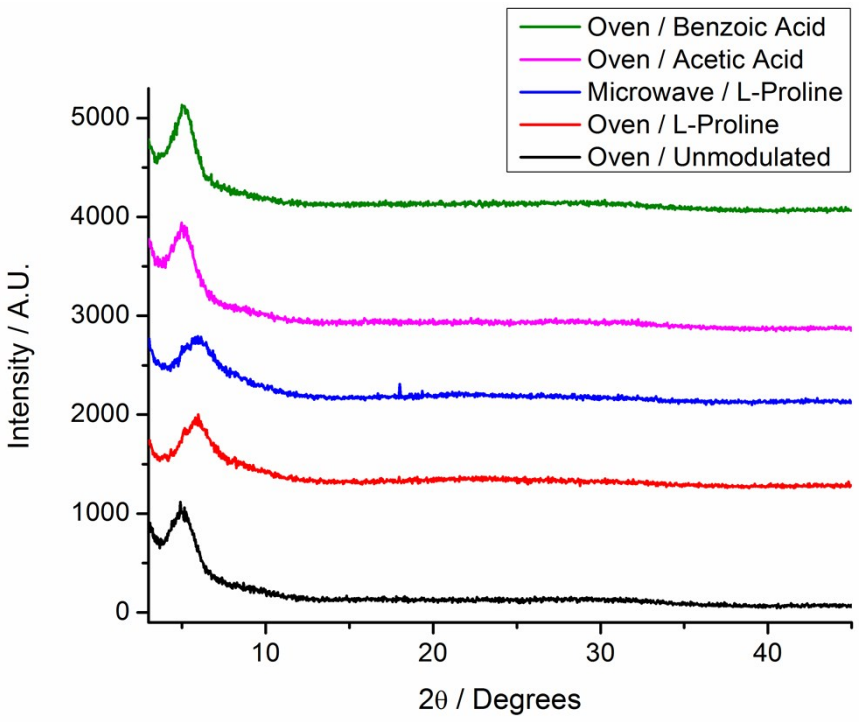

Figure S8. Powder X-ray diffraction analyses of attempts to synthesise a Zr MOF from the edtb linker. The key gives the heating conditions and modulator used in the synthesis attempt.

S8. References

S1. C. F. Macrae, I. J. Bruno, J. A. Chisholm, P. R. Edgington, P. McCabe, E. Pidcock, L. Rodriguez-Monge, R. Taylor, J. van de Streek and P. A. Wood, *J. Appl. Cryst.*, 2008, **41**, 466–470.

S2. T. Gadzikwa, B.-S. Zeng, J. T. Hupp and S. T. Nguyen, *Chem. Commun.*, 2008, 3672–3674.

S3. M. Belema and P. Hewawasam, *U.S. Pat.* US20110237636A1, 2011.

S4. Bruker (2007). Bruker AXS Inc., Madison, Wisconsin, USA.

S5. Bruker (2012). Bruker AXS Inc., Madison, Wisconsin, USA.

S6. L. Palatinus, G. Chapuis, *J. Appl. Cryst.* 2007, **40**, 786–790.

S7. G. M. Sheldrick, *Acta Cryst.* 2008, **A64**, 112–122.

S8. O. V. Dolomanov, L. J. Bourhis, R. J. Gildea, J. A. K. Howard and H. Puschmann, *J. Appl. Cryst*. 2009, **42**, 339–341.

S9. R. J. Marshall, S. L. Griffin, C. Wilson, R. S. Forgan, *J. Am. Chem. Soc.,* 2015, **137**, 9527–9530.

S10. CrysAlisPro, Agilent Technologies, Version 1.171.37.35 (release 13-08-2014 CrysAlis171 .NET) (compiled Aug 13 2014, 18:06:01).

S11. P. W. Betteridge, J. R. Carruthers, R. I. Cooper, K. Prout, D. J. Watkin, *J. Appl. Cryst.* 2003, **36**, 1487.

S12. A. L. Spek, *Acta Cryst.* 2015, **C71**, 9–18.

S13. CrystalClear-SM Expert 3.1 b27 (Rigaku, 2012).

S14. W. C. Oliver and G. M. Pharr, *J. Mater. Res*., 2004, **19**, 3–20.